

# Water Hydrogen-Bonding Network Structure and Dynamics at Phospholipid Multibilayer Surface: Femtosecond Mid-IR Pump–Probe Spectroscopy

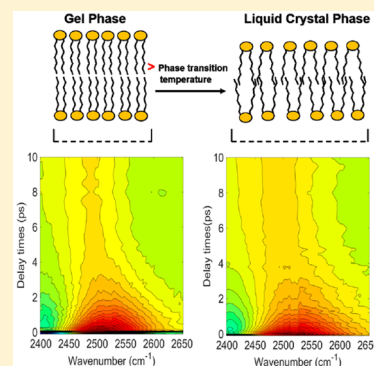
Achintya Kundu,<sup>†,‡</sup> Bartosz Błasiak,<sup>†,‡</sup> Joon-Hyung Lim,<sup>†,‡</sup> Kyungwon Kwak,<sup>§</sup> and Minhaeng Cho<sup>\*,†,‡</sup>

<sup>†</sup>Center for Molecular Spectroscopy and Dynamics, Institute for Basic Science (IBS) and <sup>‡</sup>Department of Chemistry, Korea University, Seoul 136-701, Republic of Korea

<sup>§</sup>Department of Chemistry, Chung-Ang University, Seoul 156-756, Republic of Korea

## S Supporting Information

**ABSTRACT:** The water hydrogen-bonding network at a lipid bilayer surface is crucial to understanding membrane structures and its functional activities. With a phospholipid multibilayer mimicking a biological membrane, we study the temperature dependence of water hydrogen-bonding structure, distribution, and dynamics at a lipid multibilayer surface using femtosecond mid-IR pump–probe spectroscopy. We observe two distinguished vibrational lifetime components. The fast component (0.6 ps) is associated with water interacting with a phosphate part, whereas the slow component (1.9 ps) is with bulk-like choline-associated water. With increasing temperature, the vibrational lifetime of phosphate-associated water remains constant though its relative fraction dramatically increases. The OD stretch vibrational lifetime of choline-bound water slows down in a sigmoidal fashion with respect to temperature, indicating a noticeable change of the water environment upon the phase transition. The water structure and dynamics are thus shown to be in quantitative correlation with the structural change of liquid multibilayer upon the gel-to-liquid crystal phase transition.



The biological membrane is the boundary of a biological cell. One of the main components of the biological membrane is phospholipids. These molecules spontaneously self-assemble into a bilayer upon contact with water. Water in the vicinity of its hydrophilic head part is very important for the functional activity of the membrane proteins. For example, several recent studies showed that voltage-sensitive proteins work only when water molecules at the membrane surface intimately interact with protein.<sup>1</sup> Even in the absence of membrane-bound proteins, water also plays an important role in maintaining a membrane's structural integrity and functional activities.<sup>2</sup> Water structure at the lipid/water surface has been extensively studied by vibrational sum frequency generation.<sup>3,4</sup> It is well established that there exist different types of water molecules at the zwitterionic lipid/water surface: (1) phosphate-bound water, (2) choline-bound water, and (3) hydrophobic water. Water dynamics at the lipid/water surface was also studied by femtosecond mid-IR pump–probe<sup>5</sup> and time-resolved vibrational sum frequency generation spectroscopy.<sup>6</sup> It is commonly observed that there are two significantly different vibrational lifetime components, which have been assigned to phosphate-bound water and bulk-like choline-associated water.

The fluidity of the gel phase of the membrane differs from that of the liquid crystal phase, which suggests that the lipid–water interaction at the gel phase is different from that of the liquid crystal phase.<sup>7</sup> Up to now, all of the measurements have mainly concentrated on measuring the effect of changing the

hydration level with water concentration as a control variable. However, there is no ultrafast vibrational spectroscopic study on water structure and dynamics with changing the structure of the membrane. Therefore, it is important to study water hydrogen-bonding structure and dynamics at the different phases.

The phase transition from the gel phase to the liquid crystal phase can be realized by changing temperature.<sup>8,9</sup> Depending on temperature, the packing of the lipid bilayer will change. At lower than phase transition temperature, all the lipid molecules are closely packed, and the hydrophobic chains are fully extended. On the other hand, at higher than phase transition temperature, the lipid molecules are not fully extended any more, surface area increases, and bilayer thickness decreases. The structures of the lipid bilayer below and above the phase transition temperature are schematically shown in Figure 1a. Previously a different model system was used to study the structural and functional activity of the membrane.<sup>10–16</sup> Here, we prepared phospholipid multibilayers as a model system, and employed femtosecond mid-IR pump–probe method with HOD infrared probing to study the water hydrogen-bonding network and dynamics.

**Received:** January 5, 2016

**Accepted:** February 9, 2016

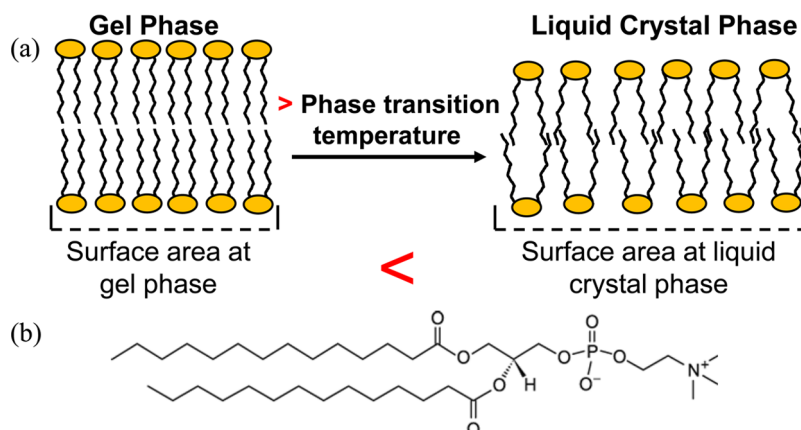


**Figure 1.** (a) Sketch of a model biological membrane below and above the phase transition temperature. (b) Chemical structure of a zwitterionic lipid DMPC.

The phospholipid multibilayer studied here is produced by zwitterionic 1,2-dimyristyl-*sn*-glycero-3-phosphocholine (DMPC) molecules (see Figure 1b). We used DMPC because this lipid forms very stable multibilayers<sup>5,17</sup> and its phase (gel  $\rightarrow$  liquid crystal) transition temperature is around room temperature (297 K).<sup>18</sup> Therefore, we can easily control the temperature above and below the phase transition temperature. The lipid multibilayer was prepared between two 3 mm thick CaF<sub>2</sub> windows as described by the Fayer group.<sup>5,17</sup> The molar ratio of the lipid to water was 16. At this low hydration level, most water molecules are close to the phosphate and choline parts of the lipid multibilayers. The measurement was done with IR probing of the OD stretch mode of diluted HOD in H<sub>2</sub>O to avoid complication from resonant vibrational excitation transfer between probe modes.<sup>19,20</sup> The time-resolved IR pump-probe (IR PP) spectra of the OD stretch mode at this lipid multibilayer were measured by femtosecond mid-IR pump-probe.

Figure 2a shows the background-subtracted and normalized linear absorption spectrum of OD stretch mode. The red and

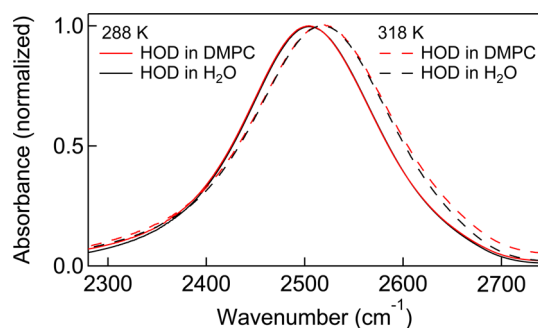
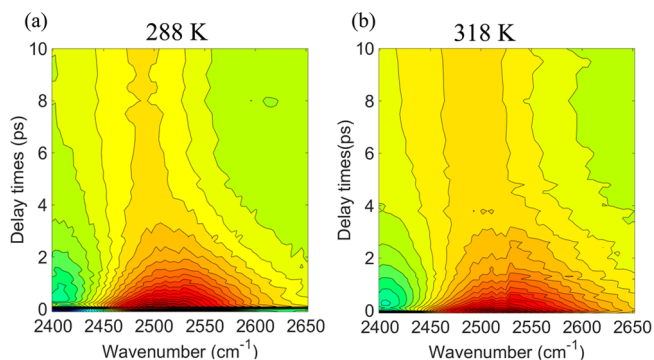


**Figure 2.** Background-subtracted peak-normalized linear FTIR spectra of the OD stretch mode of HOD probe molecules in a DMPC multibilayer and in isotopically diluted bulk water at two different temperatures.

black lines are the linear absorption spectra of the OD stretch mode of HOD in DMPC multibilayer solution and that in the isotopically diluted bulk water, respectively. The solid and dashed lines are the spectra at 288 and 318 K, respectively. The absorption spectra of the OD stretch mode in the DMPC multibilayer are indistinguishable from that in the isotopically diluted bulk water. The main spectral feature with increasing

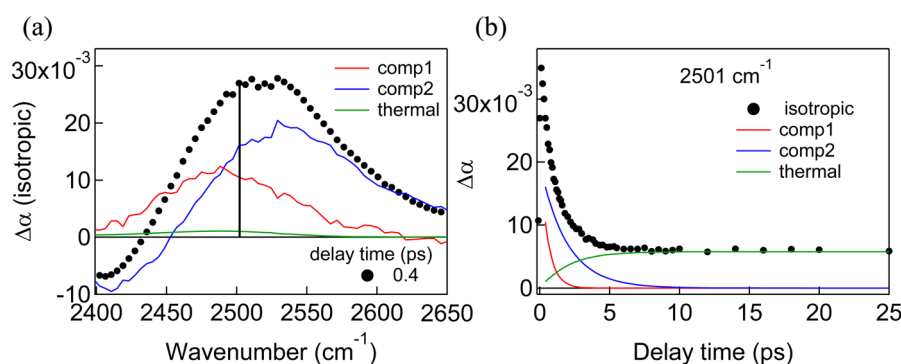
temperature from 288 to 318 K is blue shifting of the peak position. This indicates the reduction in the number of water H-bonds or the weakening of the H-bond network in the DMPC multibilayer. Similarly, the blue shift of peak position was also observed for bulk water when temperature was increased.<sup>21</sup>

Figure 3a,b shows the isotropic IR PP spectra of the OD stretch of HOD in the DMPC phospholipid multibilayer at 288



**Figure 3.** Isotropic IR PP signals of the OD stretch mode of HOD probe molecules in a lipid multibilayer at 288 K (a) and 318 K (b), respectively.

and 318 K, respectively. The IR PP signal shows both positive (red) and negative (green) features at early times (up to 4 ps). After that, there is only positive signal. The positive signal in the IR PP spectrum corresponds to the ground state bleach and stimulated emission (0–1 transition) contribution, whereas the negative signal is due to the excited state absorption (1–2 transition). It is clear that the signal on the low-frequency (red) side decays faster than that on the blue side (see Supporting Information (SI)), which indicates at least two different vibrational lifetime components. The IR PP spectra decay up to  $\sim$ 8 ps with two different vibrational lifetime components, but after 8 ps the signal remains constant (see Figure S2). At long times ( $>$ 8 ps), the positive bleaching signal is due to the increase in local temperature, which is caused by the pump pulse.<sup>22,23</sup> The peak position of the bleaching signal is blue-shifted by 10 cm<sup>-1</sup> with increasing temperature and the intensity of the IR PP signal decreases due to the non-Condon effect (see Figure S2).<sup>24</sup>



**Figure 4.** (a) Decomposition of the IR PP spectrum (0.4 ps, black circles) into two decay components (comp1: red; comp2: blue) and a growing heating component (thermal: green) at 288 K. (b) Black circles are time dependence decay of an isotropic IR PP signal at 2501  $\text{cm}^{-1}$ . Red and blue lines are kinetic traces at 2501  $\text{cm}^{-1}$  of comp1 and comp2, respectively. The green line represents the growing heating component.

From the above discussion, it is clear that the time-dependence of IR PP spectra can be explained by considering at least three spectral components: two decaying components, and one rising heating component. We have analyzed the IR PP spectra with a model proposed by Bakker and co-workers,<sup>22,23</sup> which takes into account the effects of both the ingrowing heating component and the two decaying components.

Figure 4a shows the total IR PP spectrum (black circles) at 0.4 ps and the corresponding eigen spectra of the two decaying components, comp1 (red) and comp2 (blue), and the heating component, thermal (green) at 288 K. The peak position of comp1 is red-shifted with respect to that of comp2. Figure 4b depicts the temporal profiles of comp1, comp2, and thermal component at 2501  $\text{cm}^{-1}$ . The black circles in Figure 4b represent the time-resolved IR PP signal at 2501  $\text{cm}^{-1}$ . Comp1 decays much faster than comp2, and its vibrational lifetime is 0.6 ps, whereas that of comp2 is 1.9 ps. The center peak position of comp1 is at 2490  $\text{cm}^{-1}$ , which is much lower in frequency than that (OD band) of HOD in water. Furthermore, its line-width is narrower than that of bulk water. As the negatively charged phosphate creates a large electric field at the associated OD, the peak position of comp1 is red-shifted with respect to bulk water.<sup>5</sup> Thus comp1 can be assigned to water molecules associated with phosphate group of the lipid, which is consistent with the previous assignment by Zhao et al.<sup>5</sup> and Bonn et al.<sup>6</sup> The vibrational lifetime of comp2 is close to that of bulk water. Therefore, comp2 is the spectrum of bulk-like choline-associated water.

Now, Figure 5a,b shows the entire spectra of comp1 and comp2 at different temperatures, respectively. Comp1 shows only the bleaching signal in this frequency range. The peak frequency of the comp1 spectrum is significantly blue-shifted (from  $\sim 2490 \text{ cm}^{-1}$  at 288 K to 2520  $\text{cm}^{-1}$  at 318 K), and its T-dependence shows a sigmoidal pattern (Figure 5c). As temperature increases, the surface area of the lipid bilayer increases, and more water molecules can access the phosphate part as the multibilayer undergoes a gel-to-liquid crystal phase transition (shown in Figure 5d). Figure 5d exhibits the dramatic changes of the relative fractions of the two different types of water molecules upon the phase transition, which were extracted from the integrated areas of the pump–probe spectra with the assumption that the OD transition dipole moment is approximately frequency-independent. This strongly shows that the redistribution of the water H-bonds occurs at the phase transition point, though the H-bond strength of OD with a phosphate group remains the same (note that the supporting

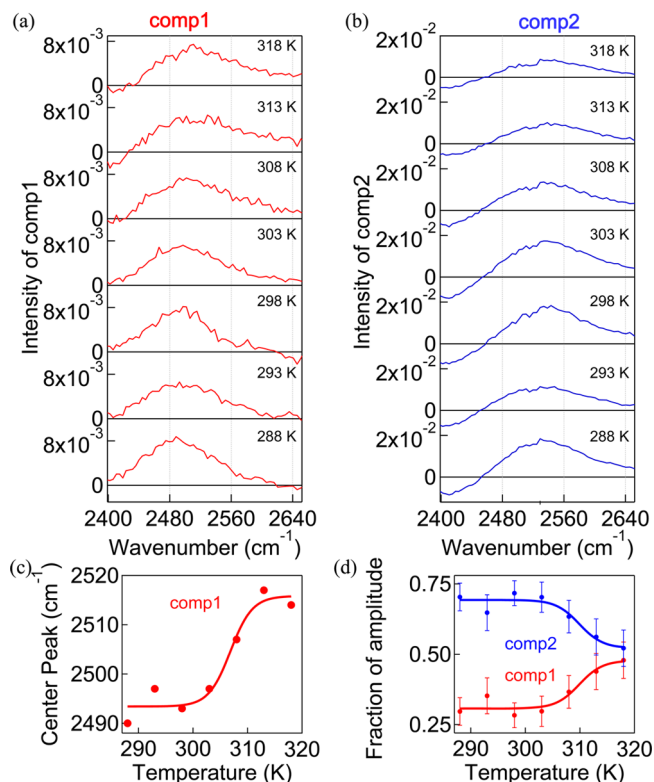


**Figure 5.** Decomposed comp1 and comp2 at different temperatures. (a) Comp1 is phosphate-associated water. (b) Comp2 is choline-associated bulk water. (c) Temperature dependence of peak position of comp1. (d) Fractions of the amplitudes of the two decay components with respect to temperature. The red and blue lines are guides to the eye.

evidence for this statement will be discussed later with Figure 6). More specifically, the sigmoidal (blue-shifting) change of comp1 peak frequency with increasing temperature indicates either reduction of the H-bond number around the HOD of HOD...OP complex or weakening of the corresponding H-bond. Comp2 exhibits both positive bleaching signal at 2500  $\text{cm}^{-1}$  and negative excited state absorption at 2410  $\text{cm}^{-1}$ . Although the bleaching signal is slightly blue-shifted with increasing temperature, it is difficult to accurately estimate the magnitude of such a blue shift because the bleaching signal overlaps with the excited state absorption.

Figure 6a shows the two vibrational lifetimes,  $\tau_1$  (comp1) and  $\tau_2$  (comp2), and that of the OD stretch mode in

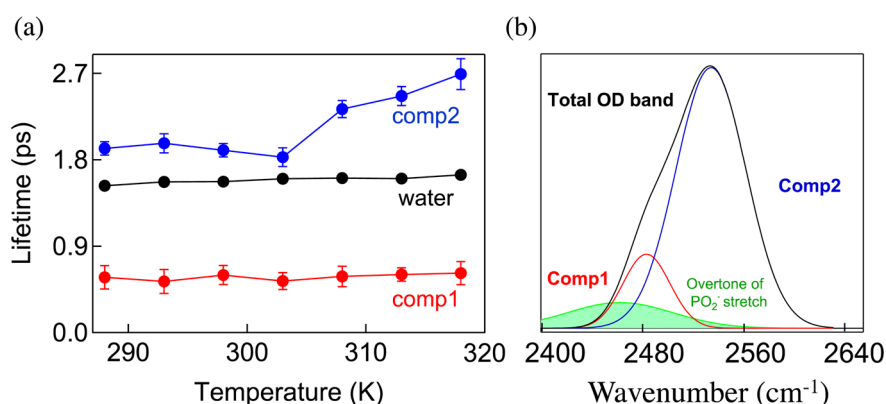


**Figure 6.** (a) The vibrational decay time constants for two decay components (comp1: red; comp2: blue) in DMPC multibilayer and in isotopically diluted bulk water as a function of temperature. (b) Schematic representation of two different components of the OD stretch mode and overtone bands of an asymmetric phosphate ( $\text{PO}_2^-$ ) stretch.

isotopically diluted bulk water at different temperatures. It is known that the vibrational lifetime is sensitive to the local environment and the anharmonic couplings with intramolecular vibrational modes. The existence of two vibrational lifetime components was observed for the lipid/water surface,<sup>5</sup> nanoscopic water channels of nafen membranes,<sup>25</sup> and lipid reverse micelles.<sup>26</sup> Here, we also observed the fast (comp1) and slow (comp2) components at the lipid multibilayer. The vibrational lifetime of comp1 is constant throughout the experimental temperature range, but the vibrational lifetime of comp2 increases from 1.9 to 2.5 ps at around 307 K. The vibrational lifetime of OD stretch in isotopically diluted water is barely temperature dependent in this temperature range.

The dominant pathway of the vibrational relaxation of the OD stretch mode is through the overtone band of an asymmetric phosphate ( $\text{PO}_2^-$ ) stretch mode<sup>27</sup> and the fundamental of an HOD bend mode.<sup>21</sup> The vibrational density of states (VDOS) of the overtone of the asymmetric phosphate stretch band is close to the OD stretch mode (see Figure S1). Therefore, the observation in Figure 6a suggests that, as schematically shown in Figure 6b, the VDOS of the overtone band of asymmetric phosphate stretch mode overlaps with the comp1 spectrum, which might lead to the very fast vibrational relaxation of comp1.<sup>27</sup> The fact that the vibrational lifetime of comp1 is constant throughout the temperature range, even though comp1 is blue-shifted with increasing temperature, can be explained by noting that the spectral overlap between the comp1 spectrum and VDOS of the overtone of the asymmetric phosphate stretch mode changes little as the asymmetric phosphate stretch IR spectrum is independent of the temperature (see Figure S1) and the comp1 spectrum is almost at the center of the VDOS of the asymmetric phosphate stretch overtone mode.

The vibrational lifetime of comp2,  $\tau_2$ , is constant below the phase transition temperature, but it suddenly increases at 307 K. Above this temperature,  $\tau_2$  gradually increases with increasing temperature. At lower temperatures (below phase transition temperature), because of tight packing of the head part of the lipid in the gel phase, mainly bulk-like water around the choline part contributes to comp2, and the vibrational lifetime ( $\sim 1.9$  ps) is indeed close to bulk water ( $\sim 1.5$  ps). As temperature increases from 303 to 308 K, the vibrational lifetime  $\tau_2$  jumps from 1.9 to 2.3 ps. This sudden increase of the vibrational lifetime has not been observed before. With increasing temperature, a lipid phase transition from the gel

phase to the liquid crystal phase occurs. Because of the concomitant structural change of the lipid bilayer, the water molecules near the more hydrophobic choline part contribute to comp2. This might be the reason that the vibrational lifetime  $\tau_2$  of comp2 shows a discontinuous jump at the phase transition temperature (same temperature that we observed in Figure 5c). The increased vibrational lifetime with increasing temperature beyond the phase transition temperature can be explained by the heating effect of the water dynamics.<sup>28</sup> The vibrational energy of the OD stretch mode of the comp2 is transferred to the fundamental HOD bending mode and an additional excitation of lower energy modes<sup>29</sup> (fundamental HOD bend frequency is at 1450  $\text{cm}^{-1}$ ). With increasing temperature, the OD stretch vibration is blue-shifted, which increases the energy gap between the OD stretch mode and the fundamental HOD bending mode. As a consequence, the vibrational relaxation rate of the OD stretch mode of comp2 is slowed down with increasing temperature.<sup>28</sup> Upon T-induced phase transition, the water structures near both phosphate and choline parts change as evidently shown in the sigmoidal patterns of the peak frequency of comp1 (Figure 5c) as well as of the vibrational lifetime of comp2 (Figure 6a).

In summary, we used the femtosecond mid-IR pump-probe method to study water structure and dynamics at two different (gel and liquid crystal) phases of aligned phospholipid multibilayer systems. We observed two very different vibrational lifetime components at each phase of the lipid multibilayer. The component with long lifetime can be assigned to the OD vibrational relaxation of bulk-like choline-bound water molecules, whereas that with short lifetime originates from phosphate-bound water. The vibrational lifetime of the former increases when the multibilayer undergoes a temperature-induced phase transition, indicating changes of water H-bonding structure. On the other hand, the vibrational lifetime of the phosphate-bound water is constant regardless of the structural phase transition of the lipid multibilayer, even though the relative population of phosphate-bound water molecules dramatically increases upon the corresponding phase transition. It is believed that such tightly phosphate-bound water molecules surviving over the lipid bilayer phase-transition could play an important role in biological processes, since they are directly involved in fast proton transfer at the membrane surface. Here we provide a mechanistic explanation of the temperature-dependent vibrational lifetime of the OD stretch mode of HOD and more importantly show the redistribution of

water molecules in a lipid multibilayer system at a temperature-induced phase transition point.

## ■ ASSOCIATED CONTENT

### ● Supporting Information

The Supporting Information is available free of charge on the ACS Publications website at DOI: 10.1021/acs.jpcllett.6b00022.

Details of the experiments and the data analyses. Supporting Information file contains the following sections (1) Sample, (2) FTIR Measurement, (3) Femtosecond Mid-IR Pump–Probe Spectroscopy, and (4) References (PDF)

## ■ AUTHOR INFORMATION

### Corresponding Author

\*E-mail: mcho@korea.ac.kr.

### Notes

The authors declare no competing financial interest.

## ■ ACKNOWLEDGMENTS

This work was supported by IBS-R023-D1. All IR PP measurements were performed by using the multidimensional spectroscopy facility in the Seoul Center of Korea Basic Science Institute (KBSI).

## ■ REFERENCES

- (1) Krepiy, D.; Mihailescu, M.; Freitas, J. A.; Schow, E. V.; Worcester, D. L.; Gawrisch, K.; Tobias, D. J.; White, S. H.; Swartz, K. J. Structure and Hydration of Membranes Embedded with Voltage-Sensing Domains. *Nature* **2009**, *462*, 473–479.
- (2) Murzyn, K.; Pasenkiewicz-Gierula, M. Structural Properties of the Water/Membrane Interface of a Bilayer Built of the E. Coli Lipid A. *J. Phys. Chem. B* **2015**, *119*, 5846–5856.
- (3) Mondal, J. A.; Nihonyanagi, S.; Yamaguchi, S.; Tahara, T. Three Distinct Water Structures at a Zwitterionic Lipid/Water Interface Revealed by Heterodyne-Detected Vibrational Sum Frequency Generation. *J. Am. Chem. Soc.* **2012**, *134*, 7842–7850.
- (4) Re, S.; Nishima, W.; Tahara, T.; Sugita, Y. Mosaic of Water Orientation Structures at a Neutral Zwitterionic Lipid/Water Interface Revealed by Molecular Dynamics Simulations. *J. Phys. Chem. Lett.* **2014**, *5*, 4343–4348.
- (5) Zhao, W.; Moilanen, D. E.; Fenn, E. E.; Fayer, M. D. Water at the Surfaces of Aligned Phospholipid Multibilayer Model Membranes Probed with Ultrafast Vibrational Spectroscopy. *J. Am. Chem. Soc.* **2008**, *130*, 13927–13937.
- (6) Bonn, M.; Bakker, H. J.; Ghosh, A.; Yamamoto, S.; Sovago, M.; Campen, R. K. Structural Inhomogeneity of Interfacial Water at Lipid Monolayers Revealed by Surface-Specific Vibrational Pump-Probe Spectroscopy. *J. Am. Chem. Soc.* **2010**, *132*, 14971–14978.
- (7) Cameron, D. G.; Martin, A.; Mantsch, H. H. Membrane Isolation Alters the Gel to Liquid Crystal Transition of *Acholeplasma Laidlawii* B. *Science* **1983**, *219*, 180–182.
- (8) Cameron, D. G.; Martin, A.; Moffatt, D. J.; Mantsch, H. H. Infrared Spectroscopic Study of the Gel to Liquid-Crystal Phase Transition in Live *Acholeplasma Laidlawii* Cells. *Biochemistry* **1985**, *24*, 4355–4359.
- (9) Träuble, H.; Eibl, H. Electrostatic Effects on Lipid Phase Transitions: Membrane Structure and Ionic Environment. *Proc. Natl. Acad. Sci. U. S. A.* **1974**, *71*, 214–219.
- (10) Chen, X.; Wang, J.; Boughton, A. P.; Kristalyn, C. B.; Chen, Z. Multiple Orientation of Melittin Inside a Single Lipid Bilayer Determined by Combined Vibrational Spectroscopic Studies. *J. Am. Chem. Soc.* **2007**, *129*, 1420–1427.
- (11) Kundu, A.; Yamaguchi, S.; Tahara, T. Evaluation of pH at Charged Lipid/water Interfaces by Heterodyne-Detected Electronic Sum Frequency Generation. *J. Phys. Chem. Lett.* **2014**, *5*, 762–766.
- (12) Mondal, J. A.; Nihonyanagi, S.; Yamaguchi, S.; Tahara, T. Structure and Orientation of Water at Charged Lipid Monolayer/water Interfaces Probed by Heterodyne-Detected Vibrational Sum Frequency Generation Spectroscopy. *J. Am. Chem. Soc.* **2010**, *132*, 10656–10657.
- (13) Cong, X.; Poyton, M. F.; Baxter, A. J.; Pullanchery, S.; Cremer, P. S. Unquenchable Surface Potential Dramatically Enhances Cu 2+ Binding to Phosphatidylserine Lipids. *J. Am. Chem. Soc.* **2015**, *137*, 7785–7792.
- (14) Nagata, Y.; Mukamel, S. Spectral Diffusion at the Water/Lipid Interface Revealed by. *J. Am. Chem. Soc.* **2011**, *133*, 3276–3279.
- (15) van der Post, S. T.; Hunger, J.; Bonn, M.; Bakker, H. J. Observation of Separated Ion-Pairs Between Cations and Phospholipid Headgroups. *J. Phys. Chem. B* **2014**, *118*, 4397–4403.
- (16) Engel, M. F. M.; Vandenakker, C. C.; Schlegler, M.; Velikov, K. P.; Koenderink, G. H.; Bonn, M. The Polyphenol EGCG Inhibits Amyloid Formation Less Efficiently at Phospholipid Interfaces than in Bulk Solution. *J. Am. Chem. Soc.* **2012**, *134*, 14781–14788.
- (17) Kel, O.; Tamimi, A.; Thielges, M. C.; Fayer, M. D. Ultrafast Structural Dynamics Inside Planar Phospholipid Multibilayer Model Cell Membranes Measured with 2D IR Spectroscopy. *J. Am. Chem. Soc.* **2013**, *135*, 11063–11074.
- (18) Peters, G. H.; Wang, C.; Cruys-Bagger, N.; Velardez, G. F.; Madsen, J. J.; Westh, P. Binding of Serotonin to Lipid Membranes. *J. Am. Chem. Soc.* **2013**, *135*, 2164–2171.
- (19) Woutersen, S.; Bakker, H. J. Resonant Intermolecular Transfer of Vibrational Energy in Liquid Water. *Nature* **1999**, *402*, 507–509.
- (20) Verma, P. K.; Lee, H.; Park, J.-Y.; Lim, J.-H.; Maj, M.; Choi, J.-H.; Kwak, K.-W.; Cho, M. Modulation of the Hydrogen Bonding Structure of Water by Renal Osmolytes. *J. Phys. Chem. Lett.* **2015**, *6*, 2773–2779.
- (21) Nicodemus, R. A.; Ramasesha, K.; Roberts, S. T.; Tokmakoff, A. Hydrogen Bond Rearrangements in Water Probed with Temperature-Dependent 2D IR. *J. Phys. Chem. Lett.* **2010**, *1*, 1068–1072.
- (22) Rezus, Y. L. A.; Bakker, H. J. On the Orientational Relaxation of HOD in Liquid Water. *J. Chem. Phys.* **2005**, *123*, 114502–114509.
- (23) van der Post, S. T.; Bakker, H. J. The Combined Effect of Cations and Anions on the Dynamics of Water. *Phys. Chem. Chem. Phys.* **2012**, *14*, 6280–6288.
- (24) Loparo, J. J.; Roberts, S. T.; Nicodemus, R. A.; Tokmakoff, A. Variation of the Transition Dipole Moment across the OH Stretching Band of Water. *Chem. Phys.* **2007**, *341*, 218–228.
- (25) Moilanen, D. E.; Piletic, I. R.; Fayer, M. D. Water Dynamics in Nafion Fuel Cell Membranes: The Effects of Confinement and Structural Changes on the Hydrogen Bond Network. *J. Phys. Chem. C* **2007**, *111*, 8884–8891.
- (26) Lee, J.; Maj, M.; Kwak, K.; Cho, M. Infrared Pump – Probe Study of Nanoconfinement Water Structure in Reverse Micelle. *J. Phys. Chem. Lett.* **2014**, *5*, 3404–3407.
- (27) Costard, R.; Levinger, N. E.; Nibbering, E. T. J.; Elsaesser, T. Ultrafast Vibrational Dynamics of Water Confined in Phospholipid Reverse Micelles. *J. Phys. Chem. B* **2012**, *116*, 5752–5759.
- (28) Nicodemus, R. A.; Corcelli, S. A.; Skinner, J. L.; Tokmakoff, A. Collective Hydrogen Bond Reorganization in Water Studied with Temperature-Dependent Ultrafast Infrared Spectroscopy. *J. Phys. Chem. B* **2011**, *115*, 5604–5616.
- (29) Tielrooij, K. J.; Petersen, C.; Rezus, Y. L. A.; Bakker, H. J. Reorientation of HOD in Liquid H<sub>2</sub>O at Different Temperatures: Comparison of First and Second Order Correlation Functions. *Chem. Phys. Lett.* **2009**, *471*, 71–74.